11th Australasian Fluid Mechanics Conference
University of Tasmania, Hobart, Australia
14-18 December 1992

NUMERICAL INVESTIGATION OF TURBULENCE-DRIVEN SECONDARY FLOW IN A SQUARE DUCT USING AN ANISOTROPIC TURBULENCE MODEL

SONG Baojun, GU Chuangang and MIAO Yongmiao

Department of Power Machinery Engineering, Xian Jiaotong University
Xian, Shaanxi 710049, P R CHINA

Abstract

The anisotropic k—ε turbulence model is simplified by using the boundary layer approximation. And the simplified anisotropic k — ε model is compared with the Gessner' s algebraic stress model. The developing turbulent flow in a square duct involving turbulence — driven secondary flow is investigated numerically by making use of a finite volume method. The turbulence is represented by the simplified anisotropic k — ε model. The present results are compared with the detailed laser- Doppler anemometry measurements of Melling and Whitelaw.

Notation

D_h	=hydraulic diameter
k	=kinetic energy of turbulence
p	=mean pressure
Re	=Reynolds number, $\equiv D_h \cdot u_b/\nu$
$R_{11}\sim R_{33}$	=Reynolds stress components
R_{ij}	=Reynolds stress tensor
u, v, w	=mean velocity components in the x, y, and z directions, respectively.
u_b	=mean primary bulk velocity
u_i, u_j, u_a	=mean velocity tensors
u_i', u_j'	=fluctuating velocity tensors
u_s	= mean velocity along axis of square duct.
x,y,z	=coordinate axes, Fig. 1
x_i, x_j	=coordinate tensors.
δ_{ij}	=Kronecker delta
ε	=dissipation rate
ν	=kinematic viscosity
ν_e	=turbulence viscosity
μ_t	=coefficient of viscosity
ρ	=fluid density.

Introduction

As representative turbulence model, there exist the large—eddy simulation (Rogallo and Moin, 1984), stress (Launder, et al, 1975) and k—ε model. In engineering problems, the k—ε model based on an isotropic eddy—viscosity representation for the Reynolds stress is widely used, mainly due to short computing times and the simplicity of model. However, owing to the intrinsic isotropic property of the k— ε model, it can not predict accurately the complex turbulent flows subjected to extra rates of strain which are caused by the wall, curvature and Coriolis force. In order to overcome the difficulties of the k — ε model, various types of stress models have been developed. In those models, no use is made of an eddy viscosity representation for the Reynolds stress. Hence the stress model can more accurately predict the complex turbulent flows. In the calculations of the flows with three — dimensional flows, however, the number of flow quantities in the stress models increase significantly compared with the k—ε model. In order to make the k—ε model be more universal, Nisizima and Yoshizawa (1989) have proposed an anisotropic k — ε model based on the statistical results, and numerically investigated the turbulent channel and Couette flows.

The turbulent flow in a straight duct is a typical example of complex turbulent flows. This flow is accompanied by the secondary motion in the plane perpendicular to the streamwise direction, and this secondary motion is caused by turbulence. Fully — developed turbulent flow in square ducts was studied by Gessner and Jones (1965), Melling and Whitelaw (1976), among others. Melling and Whitelaw performed detailed experiments for fully—developed flow using laser-Doppler anemometry, and were the first to describe the axial velocity field distribution in detail. The first calculation of secondary flow in a square duct was carried out by Launder and Ying (1973). Improved calculations were performed by Gessner and Emery (1976), Demuren and Rodi (1984) by using the nonlinear algebraic stress

model.

In the present paper, the anisotropic k — ε model (Nisizima and Yoshizawa, 1989) is simplified by using the boundary layer approximation. The comparison of the simplified anisotropic k — ε model with Gessner' s model (Gessner and Emery, 1976) is made. The developing turbulent flow in a square duct is numerically investigated by using the finite — volume difference method. The comparisons of the present results with experimental data are made.

Anisotropic k — ε Model and Its Simplification and Analysis.

The ensemble—mean equations of motion for steady-state, incompressible and turbulent flow can be written in Cartesian tensor notation as follows:

$$\frac{\partial u_i}{\partial x_i} = 0 \tag{1}$$

$$\frac{\partial u_i u_j}{\partial x_i} = -\frac{1}{\rho}\frac{\partial p}{\partial x_j} + \frac{\partial}{\partial x_i}(R_{ij} + \nu\frac{\partial u_j}{\partial x_i}) \tag{2}$$

where ν is the kinematic viscosity, R_{ij} the Reynolds stress defined as:

$$R_{ij} = -\langle u_i' u_j' \rangle \tag{3}$$

by using the ensemble mean $\langle\ \ \rangle$.

In the anisotropic k — ε model (Nisizima and Yoshizawa, 1989), R_{ij} may be expressed in the form:

$$R_{ij} = -\frac{2}{3}k\delta_{ij} + \nu_e\left(\frac{\partial u_i}{\partial x_j} + \frac{\partial u_j}{\partial x_i}\right) + \frac{1}{3}\left(\sum_{m=1}^{3}\tau_m S_{maa}\right) + R'_{ij} \tag{4}$$

where ν_e is given by

$$\nu_e = c_\mu \cdot k^2/\varepsilon \tag{5}$$

and

$$\tau_m = c_{\tau m}k^3/\varepsilon^2 \tag{6}$$

$$R'_{ij} = -\sum_{m=1}^{3}\tau_m S_{mij} \tag{7}$$

$$s_{1ij} = \frac{\partial u_i}{\partial x_a}\cdot\frac{\partial u_j}{\partial x_a} \tag{8}$$

$$s_{2ij} = \frac{1}{2}\left(\frac{\partial u_i}{\partial x_a}\cdot\frac{\partial u_a}{\partial x_j} + \frac{\partial u_j}{\partial x_a}\cdot\frac{\partial u_a}{\partial x_i}\right) \tag{9}$$

$$s_{3ij} = \frac{\partial u_a}{\partial x_i}\cdot\frac{\partial u_a}{\partial x_j} \tag{10}$$

where $c_{\tau m}$ are constants (m = 1, 2, 3) k is the turbulent kinetic energy, and ε the dissipation rate of k. They are determined from their own transport equations, that is

$$u_i\frac{\partial k}{\partial x_i} = R_{ij}\cdot\frac{\partial u_j}{\partial x_i} - \varepsilon + \frac{\partial}{\partial x_i}(c_\mu k^2/\varepsilon\cdot\frac{\partial k}{\partial x_i}) \tag{11}$$

$$u_i\frac{\partial \varepsilon}{\partial x_i} = \frac{1}{2}c_{\varepsilon 1}k\cdot\left(\frac{\partial u_i}{\partial x_j} + \frac{\partial u_j}{\partial x_i}\right)^2 - c_{\varepsilon 2}\varepsilon^2/k + \frac{\partial}{\partial x_i}(c_{\varepsilon 3}k^2/\varepsilon\frac{\partial \varepsilon}{\partial x_i}) \tag{12}$$

where c_μ, $c_{\varepsilon 1}$, $c_{\varepsilon 2}$ and $c_{\varepsilon 3}$ are constants, which are usually chosen as

$$c_\mu = 0.09, c_{\varepsilon 1} = 0.13, c_{\varepsilon 2} = 1.9, c_{\varepsilon 3} = 0.069$$

The first two terms on the right—hand side of equation (4) give the familiar isotropic eddy—representation. The third and fourth terms are crucially important in expressing the anisotropy of Reynolds stress.

For the developing turbulent flow in a square duct (shown in Fig. 1), it is known that the secondary velocities v and w are two orders of magnitude less than prime velocity u (except possibly in the viscous sublayer), that ∂u/∂y and ∂u/∂z are of the same order magitude, and that ∂u/∂y and ∂u/∂z are much larger than all other mean velocity component derivatives.

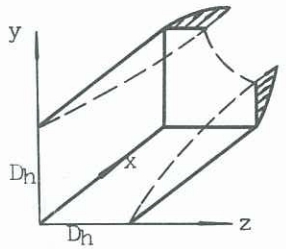

Fig. 1 Coordinate system of a square duct

If the above approximations are applied to the equation (4), simplified anisotropic Reynolds stress components are obtained by neglecting the secondary velocity gradients in the third and fourth terms in equation (4). They are given as follows:

$$R_{11} = -\frac{2}{3}k + 2\nu_e\cdot\frac{\partial u}{\partial x} + \frac{1}{3}(c_{\tau 1}+c_{\tau 3})k^3/\varepsilon^2\left[\left(\frac{\partial u}{\partial y}\right)^2 + \left(\frac{\partial u}{\partial z}\right)^2\right] \tag{13}$$

$$R_{22} = -\frac{2}{3}k + 2\nu_e\frac{\partial v}{\partial y} + \frac{1}{3}(c_{\tau 1}+c_{\tau 3})k^3/\varepsilon^2\left[\left(\frac{\partial u}{\partial y}\right)^2 + \left(\frac{\partial u}{\partial z}\right)^2\right] - c_{\tau 3}k^3/\varepsilon^2\left(\frac{\partial u}{\partial y}\right)^2 \tag{14}$$

$$R_{33} = -\frac{2}{3}k + 2\nu_e\frac{\partial w}{\partial z} + \frac{1}{3}(c_{\tau 1}+c_{\tau 3})k^3/\varepsilon^2\left[\left(\frac{\partial u}{\partial y}\right)^2 + \left(\frac{\partial u}{\partial z}\right)^2\right] - c_{\tau 3}k^3/\varepsilon^2\left(\frac{\partial u}{\partial z}\right)^2 \tag{15}$$

$$R_{12} = R_{21} = \nu_e\left(\frac{\partial u}{\partial y} + \frac{\partial v}{\partial x}\right) \tag{16}$$

$$R_{13} = R_{31} = \nu_e\left(\frac{\partial u}{\partial z} + \frac{\partial w}{\partial x}\right) \tag{17}$$

$$R_{23} = R_{32} = \nu_e\cdot\left(\frac{\partial v}{\partial z} + \frac{\partial w}{\partial y}\right) - c_{\tau 3}k^3/\varepsilon^2\frac{\partial u}{\partial y}\cdot\frac{\partial u}{\partial z} \tag{18}$$

where u is the streamwise velocity in x direction, v and w are the secondary velocities in y and z directions, respectively. Constants $c_{\tau 1}$ and $c_{\tau 3}$ are chosen as

$$c_{\tau 1} = 0.07, c_{\tau 3} = -0.015$$

according to Nisizima and Yoshizawa (1989).

The equations (11), (12) and (13)—(18) are the simplified anisotropic k — ε model. Gessner and Emery (1976) obtained an algebraic expression for Reynolds stress components by neglecting the convection and diffusion terms and by further neglecting all secondary velocity gradients in the Reynolds stress transport equation. The forms of Gessner' s model are as follows:

$$R_{22} - R_{33} = c_2 c_4 k^3/\varepsilon^2 \left[\left(\frac{\partial u}{\partial y}\right)^2 - \left(\frac{\partial u}{\partial z}\right)^2\right] \quad (19)$$

$$R_{23} = c_2 c_4 k^3/\varepsilon^2 \frac{\partial u}{\partial y} \cdot \frac{\partial u}{\partial z} \quad (20)$$

where c_2 and c_4 are constants. In the present model, (R_{22}—R_{33}) and R_{23} are given as follows:

$$R_{22} - R_{33} = -c_{\tau 3} \cdot k^3/\varepsilon^2 \left[\left(\frac{\partial u}{\partial y}\right)^2 - \left(\frac{\partial u}{\partial z}\right)^2\right] + 2\nu_e \cdot \left(\frac{\partial v}{\partial y} - \frac{\partial w}{\partial z}\right) \quad (21)$$

$$R_{23} = \nu_e \cdot \left(\frac{\partial v}{\partial z} + \frac{\partial w}{\partial y}\right) - c_{\tau 3} k^3/\varepsilon^2 \frac{\partial u}{\partial y} \cdot \frac{\partial u}{\partial z} \quad (22)$$

If the secondary velocity gradients in equations (21) and (22) are neglected, the present model is consistent with the Gessner' s model. Demuren and Rodi (1989) pointed that the secondary velocity gradients are important for the Reynolds stress relations, particularly for R_{23}. The present model has taken account into the effect of the secondary velocity gradients on Reynolds stress R_{23}.

Numerical Scheme and Boundary Conditions

All the differential equations introduced above are solved by using the finite difference method, the brief summary is provided.

(1) The computation domain is discretized, and all variables are located at the common grid position as opposed to staggered grid arrangements.

(2)Cartesian velocities are used as the variables to be solved. The fully — elliptic Navier — Stokes equations in Cartesian coordinate system (x, y, z) are discretized by following the SIMPLE method.

(3) The linkage between the continuity and the momentum equations is carried out through the pressure correction equation which is derived from the continuity and momentum equations.

(4) An effective momentum interpolation method, which links the numerical fluxes through control volume surfaces with the pressure at grid nodes, is applied to eliminate the oscillation of pressure and velocity.

the details of the numerical procedure and applications to other flow situations are given by Song Baojun (1990).

Boundary conditions need to be prescribed at entry plane, symmetry planes, exit plane and solid walls. At the entry plane of the duct, a uniform distribution of all variables is prescirbed. There the secondary velocities are set to zero and k and ε are given such small values that the eddy-viscosity ν_e is about 100 times the molecular viscosity ν. At the exit plane of the duct, the gradiecular viscosity ν. At the exit plane of the duct, the gradients normal to this plane of all the variables are set to zero, that is, the flow is developed. At the symmetry planes, the velocity component normal to symmetry plane is equal to zero, while for all other quantities, the gradients normal to this plane are taken as zero. Close to the solid walls, all the transport processes are modelled by using the wall function method. For the three — dimensional turbulent flow, the following wall functions based on the two — dimensional flow assumption are used in the near — wall region:

$$\tau_w = \frac{u_p}{y_p} \cdot \frac{\mu_l \cdot y_p^+}{\kappa^{-1} ln(E y_p^+)} \quad (23)$$

where

$$y_p^+ = (k_p \cdot c_\mu^{\frac{1}{2}})^{\frac{1}{2}} \cdot y_p/\nu \quad (24)$$

$$\varepsilon_p = (c_\mu^{\frac{1}{2}} k_p)^{\frac{3}{2}}/(k y_p) \cdot F_p \quad (25)$$

$$\left.\frac{dk}{dy}\right|_{wall} = 0 \quad (26)$$

where y is the convectional coordinate normal to the wall. The subscript p refers to the grid node next to the wall, κ and E are constants, τ_w is the reluctant wall shear stress and u_p is the reluctant velocity parallel to the wall. F_p accounts for the effects of both walls on the turbulence in the corner region (Demuren and Rodi, 1984).

The computation is performed by using a (61×21×21) uniform mesh.

Results

The calculation development of the streamwise velocity along the duct axis is shown in Fig. 2 for Re= 12000, where it is compared with the measurements of Melling and Whitelaw (1976) . It is shown that the calculated velocities rise first up to a maxium, and then decrease. This is consistent with the conclusion of Demuren and Rodi (1984). Also, it is shown that the agreement with the measured data is satisfactory.

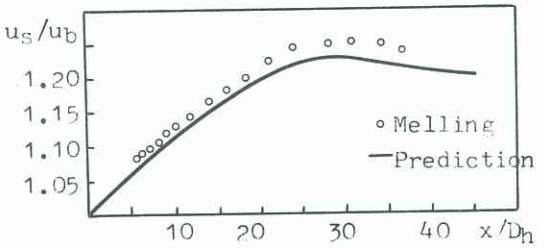

Fig. 2. Flow development along axis of the square duct

Fig. 3. (a), (b) compare calculated and measured streamwise velocity distributions along the wall and corner bisector at 36. $8D_h$. It can be seen that the present results agree with the experimental results. The discrepency between the present results with the measured data is mainly caused by the coarse graid nodes.

Due to the secondary flow associated with the turbulence, the axial velocity profile is distorted, as shown in Fig. 1. Comparison with the experimental data of Melling and Whitelaw is also shown, and the results

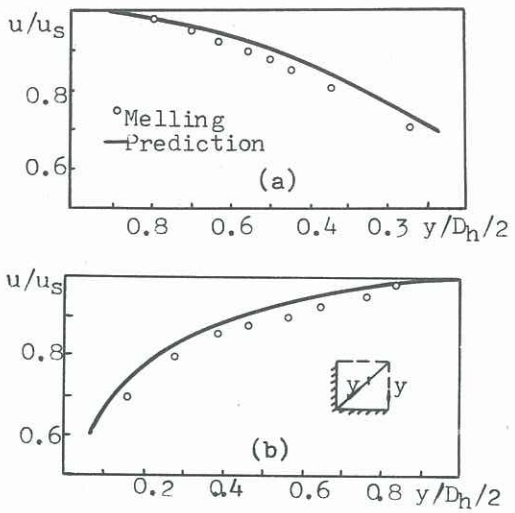

Fig. 3. Primary velocity profiles along (a) wall bisector (b) corner bisector.

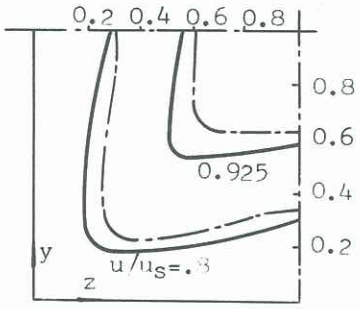

Fig. 4. Primary velocity contours (—·— Melling and Whitelaw ——— Prediction).

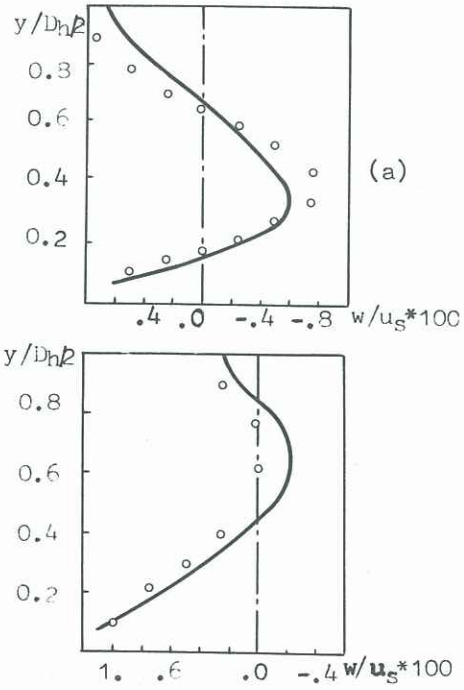

Fig. 5. Secondary velocity profiles (a) $z/D_h = 0.1$ (b) $z/D_h = 0.8$. (o Melling — Prediction)

indicate qualitatively good agreement.

The calculated secondary flow velocities at $x = 36.8D_h$ are shown in Fig. 5. It is seen that the present model can carry out the secondary flow.

Conclusion

A simplified anisotropic k—ε model has been derived according to the nature of flow in a straight duct. Through the comparison of present model with Gessner's model, it is shown that the present model can predict the turbulence—driven secondary flow in a square duct.

And the three—dimensional developing turbulent flow in a suqare duct has been numerically investigated, and the results are shown to compare well with the detailed laser—Doppler anemometry measurements of Melling and Whitelaw.

In our opinion, the anisotropic k — ε model could provide a useful alternative to a second — order closure model for complex flows. Future research should be directed toward the prediction to the flow in curved ducts using the anisotropic k—ε model.

References

Demuren, A. and Rodi,. W. (1984). Calculation of Turbulence — Driven Secondary Motion in Non — Circular Ducts, *Journal of Fluid Mechanics*, Vol. 23, pp. 689—713

Gessner, F. B. and Emery, A. F. (1976). A Reynolds Stress Model for Turbulent Corner Flows—Part I: Development of the Model. *ASME Journal of Fluids Engineering*, Vol. 98, pp. 261—268

Gessner, F. B. and Jones, J. B. (1965) On Some Aspects of Fully — Developed Turbulent Folw in Rectangular Channel. *Journal of Fluid Mechanics*, Vol. 23, pp. 689—713

Launder, B. E., Reece, G. J., and Rodi, W. (1975). Progress in the Development of a Reynolds — Stress Turbulence Closure. *Journal of Fluid Mechanics*, Vol. 68, pp. 537—566.

Melling, A. and Whitelaw, J. H. (1976) *Journal of Fluid Mechanics*. Vol. 78, pp. 289—315.

Nisizima, S. and Yoshizawa, A. (1989). Turbulent Channel and Couette Flows Using an Anisotropic k — ε Model. *AIAA Journal*, Vol. 25, No. 3, pp. 414—420.

Rogallo. R. S. and Moin, P. (1984). Numerical Simulation of Turbulent Flows. *Annual Review of Fulid Mechanics*. Vol. 16, pp. 99—137.

Song Baojun (1990). Effects of Curvature and Rotation on Internal Three—Dimensional Turbulent Flows by Method of Modified k — ε Turbulence Model. *Ph. D. Thesis*, Xi' an Jiaotong University, P. R. China